Journal of Ultrafine Grained and Nanostructured Materials
https://jufgnsm.ut.ac.ir
Vol. 56, No.1, June 2023, pp. 50-67
Print ISSN: 2423-6845 Online ISSN: 2423-6837
DOI: 10.22059/jufgnsm.2023.01.06

Friction Stir Welding/Processing of Aluminum Alloys with and without Adding Nanoparticles: A Review on the Microstructure, Texture, and Hardness

Morteza Poorghorban[1], Mohammad Yousefieh[2*], Ehsan Borhani[1]

[1]Department of Nano Technology, Nano-Materials Science and Engineering Group, Semnan University, Semnan, Iran
[2]Faculty of Materials and Metallurgical Engineering, Semnan University, Semnan, Iran.

Recieved: 23 August 2022; Accepted: 13 February 2023

**Corresponding author email: m.yousefieh@semnan.ac.ir*

ABSTRACT

Nanoscience is developing in various industrial fields, including the welding industry. On the other hand, severe plastic deformation (SPD) methods have found a special place in the world. Friction stir processing (FSP) and friction stir welding (FSW) methods are two types of severe plastic deformation (SPD) processes. In FSP and FSW, a rotating cylinder tool (pin), which could take the form of various geometries, pierces into the workpiece with a particular angle and depth. Furthermore, it refines grains by moving along with the tool's movements in the direction of interest. The uniform distribution of nanoparticles in the stir zone is one of the main challenges of using nanoparticles. Controlling variables such as tool rotational speed, tool travel speed, number of passes, etc., the distribution of nanoparticles and the grain size can be changed in the stir zone. Microstructure, texture, and grain size directly affect the hardness of the stir zone. Recent studies have shown the proper distribution of nanoparticles in the stir zone area significantly reduces the average grain size and improves the mechanical properties of the stir zone. This review aims to collect the results of previous articles focused on analyzing the operation of FSW and FSP, the microstructure of the stir zone in FSW and FSP, the impact of effective parameters on the microstructure after adding nanoparticles to the stir zone, and the applications of FSW and FSP in various industries. Moreover, the fundamental mechanisms of grain refinement throughout FSW and FSP, including morphology and grain boundaries forming, were discussed.

Keywords: *Friction stir welding, Friction stir processing, Microstructure, Hardness, Texture, Nanoparticles.*

1. Introduction

Grain refinement is one of the methods of material strength. Grain refinement methods are generally divided into thermomechanical and SPD processes. The most famous processes of SPD are ECAP, HPT, ARB, FSP, and FSW [1, 2].

Aluminum (Al) reduces environmental effects and possesses unique properties such as high specific strength, good weldability, excellent plasticity, and relatively high corrosion resistance. Therefore, it is used in different industries like structures, aviation, marine, power transmission lines, transportation, etc. Besides, aluminum alloys are competitive candidates in various complex applications [3, 4].

Aluminum is a metal extremely susceptible to grain refinement under SPD processes [1].

The high tendency of aluminum to oxidize and absorb hydrogen gas in fusion welding of aluminum alloys, defects such as porosity, inclusions in slag, and freezing cracks lower the quality and properties of the connection. On

the other hand, the production of aluminum composite by melting methods at the junction of two aluminum sheets and the production of metal-based composite will bring defects related to fusion welding and consist of unwanted reactions between the molten base metal and nanopowder. Friction stir welding was invented in England in 1991 for aluminum welding. Unlike fusion welding in FSW, the raw material will not melt, and recasting will not occur; in other words, this welding is solid-state welding. In 2001, Mishra et al., invented the FSP method to improve the surface properties of aluminum. It produces nano and micro surface composites and improves the microstructure [5-7]. The strength of 2xxx series aluminum alloys is the presence of secondary phase particles, which prevent grain growth by locking grain boundaries. Secondary phase particles are essential in preventing dislocation mobility and dynamic recovery. Since the change of strain application temperature and even the strain rate affects the sedimentation and dynamic growth of the particles, the amount of dynamic smoothness is determined by the growth of the particles during the deformation of the workpiece [8-11].

Aluminum alloys of the 6xxx series are among the precipitation-hardening alloys resulting from the heat applied by FSP/FSW; the deposits are dissolved in the disturbance region and lead to a decrease in strength in this region. Therefore, in the homogeneous and non-homogeneous connections of these alloys, the loss of strength and hardness leads to the failure of these parts at stresses lower than the tensile strength. To compensate for this loss of strength and hardness, the mechanical properties of these alloys can be improved by introducing reinforcing particles into the disturbed area and creating a composite material [11-14].

In this review paper, section 2 will briefly explain the operation of FSW and FSP. Subsequently, section 3 will investigate the microstructure of the FSW's stir zone and FSP's, the fundamental mechanism of grain refinement throughout FSW and FSP, including morphological changes and grain boundary formation, the nanoparticle distribution in the stir zone, and the effect of the texture and shape of nanoparticles in the stir zone. Section 4 examines the impact of effective parameters on the microstructure of the stir zone. Sections 5 and 6 will briefly discuss the applications of FSW and FSP in various industries and the visions and challenges concerning them in that order.

2. FSW and FSP Operation

Figure 1 demonstrates the schematic of FSW and FSP. It should be mentioned that FSP is similar to FSW [15]. FSW is a solid-state welding technique. In a solid state, the joining occurs under the melting point of base metals. In this method, the heat produced during the conversion of mechanical energy to thermal one causes structural changes and forms new grains in the stir zone. The microstructure of the stir zone includes micro and equiaxed grains made during dynamic recrystallization.

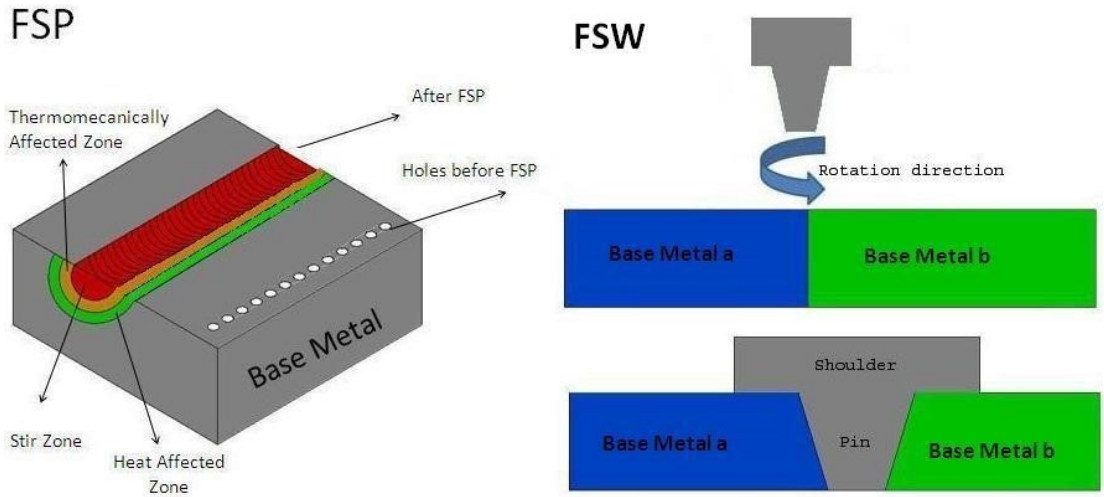

Fig. 1- The schematic of FSW and FSP methods

Material flow in FSW and FSP is complex. It is noteworthy that numerous factors could affect material flow during FSW and FSP. These factors include tool geometry (the design and dimensions of pin and shoulder), welding parameters (tool rotation and its clockwise or counterclockwise direction, traverse speed, penetration depth, the tilt angle of tools with workpiece), welded material, piece's temperature, etc. If the parameters above are not controlled, after FSW and FSP, there will be defects in and around the stir zone. These defects can be identified through destructive and nondestructive testing [16, 17]. In this light, Botes et al., [18] observed the pore or wormhole defect in the stir zone after FSP and through a scanning electron microscope (SEM) of the defect.

Rabiezadeh et al., [19] welded aluminum 5754 to aluminum 6063 by adding carbon nanotubes to the flutes of the weld zone. They reported that the hardness and strength of the welded zone were significantly higher than those of the base metal and the welded zone. FSP is similar to FSW [20]. Kishan et al., [21] prepared flutes on aluminum 6061-T6 and placed 35 nm Ti2B nanoparticles in a flute with dimensions of 1 mm and 1 mm away from the center. Following FSP, it was observed that an increase in the hardness of the stir zone of the sample had better particle distribution. Heidarpour et al., [22] made holes with a 3 mm depth and a 2 mm diameter in the middle of the workpiece with a 3 mm distance from each other in aluminum 5083, so that Al2O3 nanoparticles with a mean size of 80 nm would be placed in the holes. After FSP, it was revealed that the stir zone's hardness was greater than the base metal, owing to the appropriate distribution of nanoparticles and grain refinement.

3. Analysis of the FSW and FSP Microstructures

Grain refining is the most significant factor in hardening base metals formed through SPD. The stirring process in FSW and FSP leads to the activation of shear deformation, which produces non-directional shear texture components. This deformation leads to refining grains in the stir zone [1]. The qualitative and quantitative analyses of the stir zone can be conducted through electron backscattered diffraction (EBSD). Figure 2 depicts the colored maps of the stir zone of aluminum 7A52. In the map, the green and red lines signify the orientation of the angles wider than 15° (high angle boundaries) and the orientation of angles ranging from 2° to

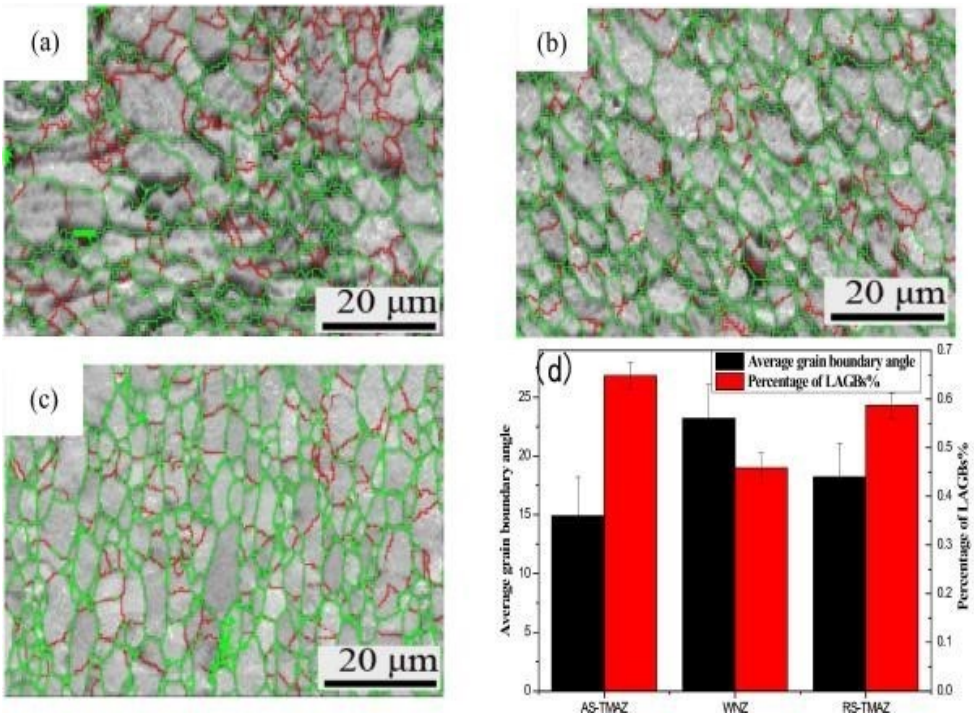

Fig. 2- Grain boundary maps: (a) AS-HAZ; (b) SZ; (c) RS-TMAZ; (d) Value of grain boundaries of 7A52 aluminum alloy FSW joint [24]

15° (low angle boundaries), respectively. Low-angle boundaries are formed during hot working with dynamic recovery [23- 24].

The motion of dislocations inside subgrains will occur following hot working. These dislocations are trapped at sub-boundaries and increase mismatch at sub-boundaries. As this process continues and the mismatch increase, sub-boundaries turn into main high-angle boundaries [25].

Three Euler angles of ϕ, φ1, and φ2 depicted in Table 1 compare the orientation distribution function (ODF) results.

SPD and the increase of temperature in FSW and FSP lead to dynamic recrystallization and changes in the substructure of the stir zone. Sarkari Khorrami et al.,[26] studied the changes in the microstructure and texture along the FSP tools on aluminum alloy 1050. As illustrated in Fig. 3, the grains are coarser and equiaxed with random orientation, more elongated, finer, and more equiaxed in front of the tools, adjacent to the tools (dotted line), and beneath the tools.

3.1. Various Recrystallization Types Created by FSW and FSP

Recrystallization requires two factors: temperature and strain or deformation. Strain rate, cooling rate, and time spent at maximum temperature are also the most influential factors in the transformation of recrystallization. Temperature also stabilizes the energy level of the grains by regularly placing the produced dislocations together, facilitating deformation, increasing strain, and reproducing the dislocations. In short, dynamic recrystallization involves the propagation of dislocations in the crystal structure of the metal and the juxtaposition of the produced dislocations, creating a boundary of sub-grains.

Continuous dynamic recrystallization (CDRX) is the gradual increase of new grains with misalignment between branches during hot plastic deformation. Continuous dynamic recrystallization consists of two stages: a) Dislocation and sub-branches formation. b) Absorption of dislocations into sub-branches and gradual increase of misalignments against discontinuous dynamic recrystallization (DDRX) The evolution of new grains in the nucleus.

Geometric dynamic recrystallization (GDRX) occurs when the grains are exposed to severe hot plastic deformation for a very long time, and the boundary of the toothed grains is blurred. These mechanisms change the microstructure of the nugget area and decompose large sediments around the nugget area.

Plastic deformation and temperature increase in the welding zone lead to dynamic recrystallization and changes in the microstructures in the stirred zone and the decomposition of sediments and coarsening around the stirred zone. Due to the severe deformation of the plastic and the sudden increase in temperature in the stirred area, the seeds break. These points are suitable points for germination. Recrystallization occurs at these points, which creates a fine-grain structure in the stirred area. In mechanical recovery, grain boundaries with a low angle are transformed into grain boundaries with a high angle, and this transformation causes the grains to enlarge. In the case of welding without the presence of reinforcing particles, the only influential factor is the temperature, or in other words, the input heat. An effective way to reduce grain size is to apply cooling methods. In welding with the presence of reinforcing particles, the principles of microstructure formation are different. On the one hand, the incoming heat increases the size of the grains. On the other hand, nano-reinforcement particles act as an obstacle to the growth of the grains and prevent them from

Table 1- Euler angles and Miller indices for essential texture components in FCC materials

Texture component	Miller indices	Euler angles		
		φ_1	Φ	φ_2
B	{1$\bar{1}$2} [110]	0	54.74	45
$\overline{\text{Bz}}$	{1$\bar{1}\bar{2}$} [$\bar{1}$ $\bar{1}$0]	0	54.74	45
C	{001} <110>	90	45	0.90
		0	90	45
Cube	{001} <100>	0.45	0	0.45
Copper	{112} <111>	90	35	45
S	{123} <634>	59	34	63

growing further, just like the seeds, known as pinning, making them finer [27-29].

Mazaheri et al., [30] reported that grain refinement increases hardness in the stir zone of aluminum grains caused by dynamic recrystallization after FSP. Singh et al., [31] added Al2O3 nanoparticles to an aluminum matrix with FSW to AA6061-T6 alloy. They realized that Al2O3 nanoparticles along the interface significantly refined the grain structure in the weld zone. This is thanks to the impact of the tin produced by Al2O3 nanoparticles which inhibits grain growth and leads to a drastic reduction in the grain size after recrystallization during FSW. LiqiangWang et al. [32] showed that the precipitation of grains could increase the dislocation density and stored energy, accelerating recrystallization.

Several researchers [33-35] believed that the microstructure of the stir zone optimizes the structure and increases the hardness due to equiaxed recrystallization during FSW.

3.2. Analyzing the Distribution of Nanoparticles in the Stir Zone

The uniform distribution of nanoparticles in the stir zone is the main challenge of using nanoparticles. Figure 4 demonstrates the distribution of particles through field emission scanning electron microscopy (FESEM).

As can be seen, FSP distributes the nanoparticles well. The distribution of nanoparticles enables extreme strain hardening of the material, which prevents local deformation and premature failure.

Every single color is assigned to one element. Nanoparticles are uniformly distributed in the stir zone, and the pin's movement prevents the particles from agglomeration [36, 37].

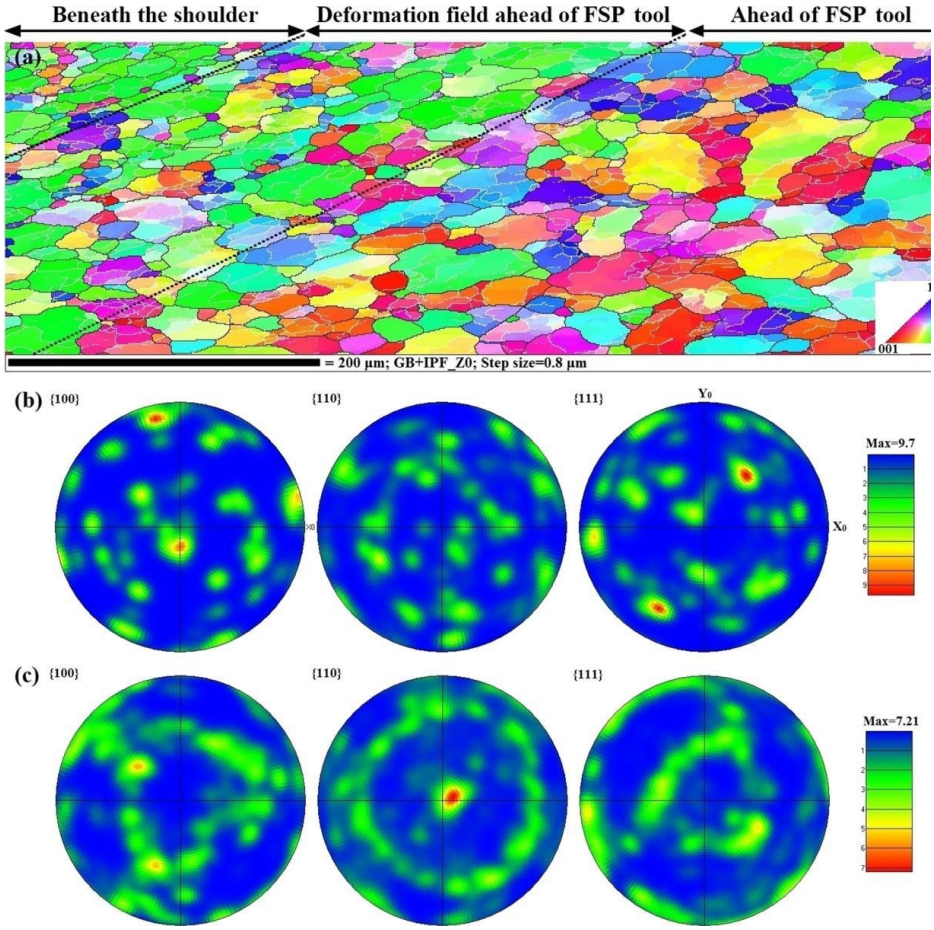

Fig. 3- (a) IPF crystal orientation map indicating the microstructure evolutions from regions in front of the FSP tool to regions beneath the shoulder; (b) and (c) (001), (110), and (111) pole figures from the front of the tool and deformation field, respectively [26].

In general, the addition of nanoparticles refines the grains in the stir zone, increases the nucleation centers during FSP, and produces the new grains. How the nanoparticles are distributed and the size of the particles can drastically affect the stir zone. Mathur et al. [38] managed to reduce the grain size through FSP, to distribute TiO2 particles in the stir zone uniformly, and to improve the hardness of the stir zone by adding TiO2 particles with a mean size of 2μm to aluminum alloy AA5052. Moustafa et al., [39] added Al2O3 and Ta2C nanoparticles with the mean size of 17.3 ± 2 nm and 280 ±4.5 nm, respectively, in addition to MWCNTs with an inside diameter of 40± 3 nm and outside diameter of 80 ±6 nm to Al2024. They found that the stir zone's hardness and mean particle size increased and decreased 30 to 40 times, respectively.

Khorrami et al., [9] reported that by adding Sic nanoparticles to aluminum 2024 by FSP, secondary nanoparticles are well distributed in the mixing area and preventing the growth and causing the formation of smaller grains. The grains are bigger in the areas where Sic nanoparticles are not distributed.

The shape and texture of nanoparticles can significantly affect the stir zone. Ostovan et al., [40] added CNT and aluminum oxide nanoparticles to aluminum 5083 through friction stir processing and distributed them uniformly in the stir zone. The microstructural analyses revealed that aluminum oxide nanoparticles disperse in different zones, including intragrain and grain boundary zones, whereas CNTs pin to grain boundaries during friction stir processing.

After the hardness test, the hardness of the stir zone in Al/Al2O3, Al/CNT, and Al/CNT/Al2O3 was estimated at around 95 HV, 110 HV, and 123 HV, respectively.

Friction stir welding and friction stir processing show a new perspective on microstructure attributable to structural modification. For this purpose, the ideal texture position can be determined by examining the texture microstructure and crystal orientation. To determine the crystal orientation,, the orientation distribution function for each sample in the Euler space at three angles of 0°, 45° and

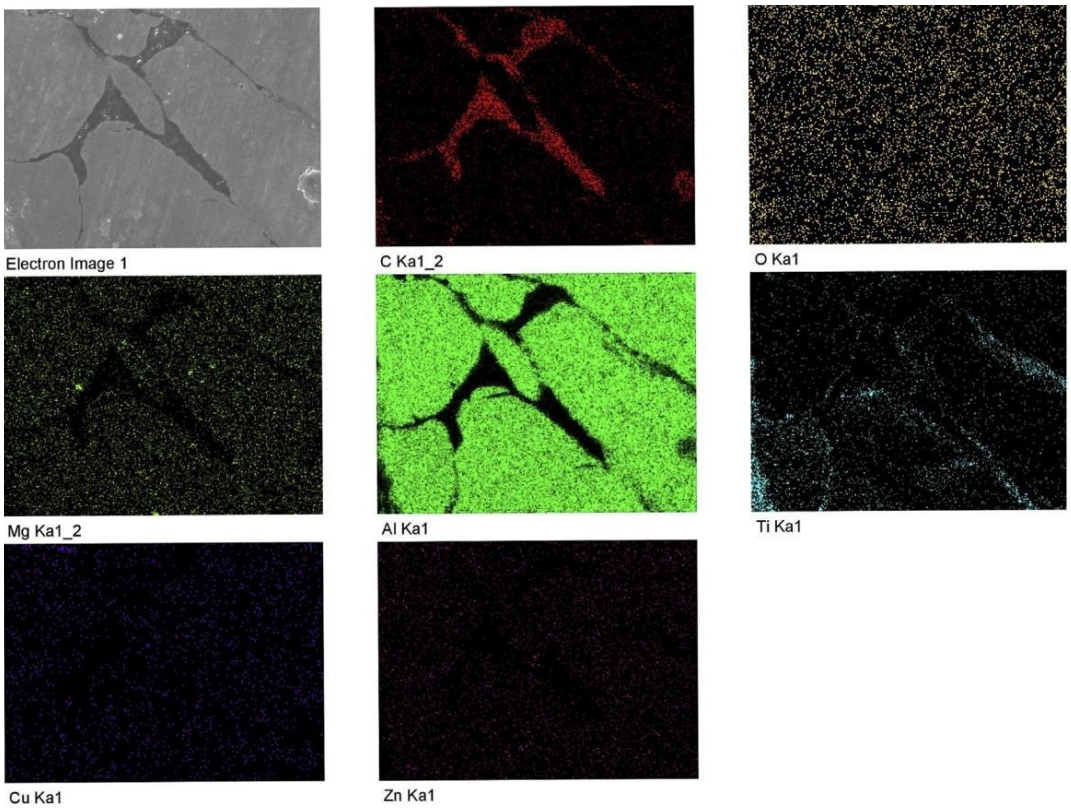

Fig. 4- The FESEM elemental mapping analysis of AA7075-TiC.Gr composite [36].

65, Figure 5 [41] can be used.

Figure 5a displays the annealing of base metal with a relatively weak cubic texture. The grains are somewhat larger and equiaxed. Figure 5b depicts the accumulative roll bonding sample in which grains are elongated along the rolling direction, creating an ultrafine grain structure. This is because the small amount of copper and S texture is created through the stir-initiated deformation. Figure 5c shows the stir zone after FSW, where the grain size in the stir zone is bigger and more equiaxed to that of Figure 5b. These equiaxed grains root back to the continuous dynamic recrystallization during FSW. The strong texture of B and the absence of a rotated cube texture indicate the occurrence of continuous dynamic recrystallization.

By using a scanning electron microscope to compare the microstructure of the annealed sample with the microstructure of the friction stir processing sample after friction stir welding, we can draw conclusions in Figure 6. [42].

figure (6a-6c) demonstrates microstructural properties based on grain structures in optical microscopy, electron backscattered diffraction maps, and the pole figure analysis of textures. The annealed sample has relatively larger grains in various directions. There is no preferred crystal

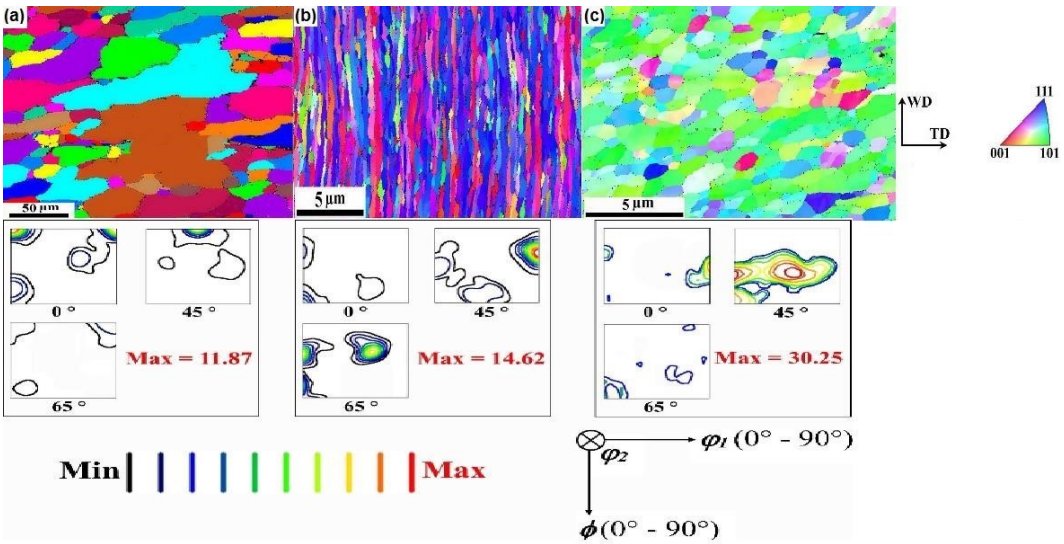

Fig. 5- The images of the electron backscatter diffraction and the orientation distribution function for a) raw specimen, b) accumulative roll bonding specimen, and c) stir zone in the joint specimen [41].

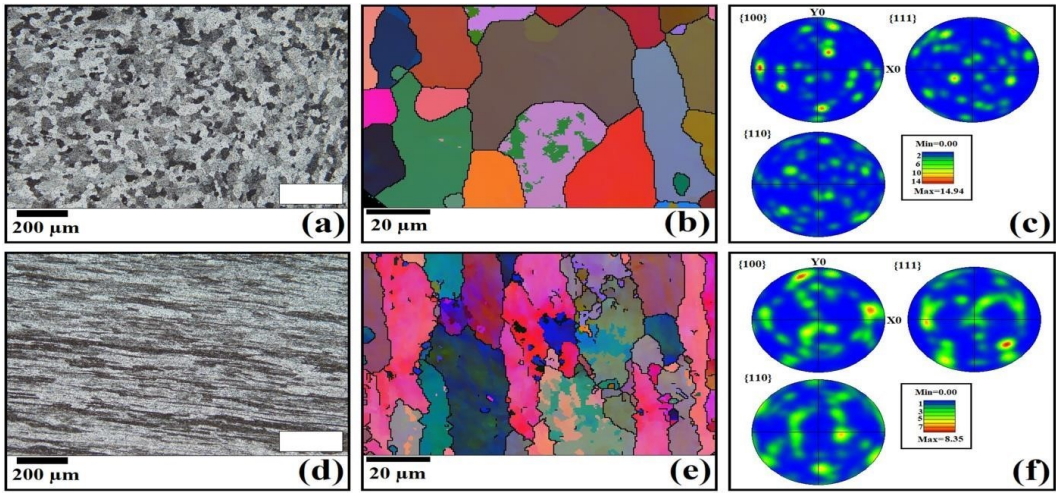

Fig. 6- Images (a-c) of Al-Mg heat treatment, images (d-f) after FSP, images (a-d) of a microscope, images (b-e) of the Euler orientation map of EBSD, and images (c-f) of the pole figure textural orientation maps [42].

orientation, and the abovementioned material is isotropic. However, the grain size is smaller in the friction stir processing sample, and the grain orientation is aligned. This indicates that the material has texture and an increase of hardness in the stir zone. As shown in d-e, the grains are elongated along the roller, and the grain boundary angle is low. Based on c-f, minor changes in the texture can be seen in the PF diagram, indicating the preferred orientation of temperature.

4. Parameters Affecting the Microstructure and the Distribution of Nanoparticles in FSW and FSP

a) The tool rotational speed (rpm): Figures 7 and 8 depict the Vickers hardness test and

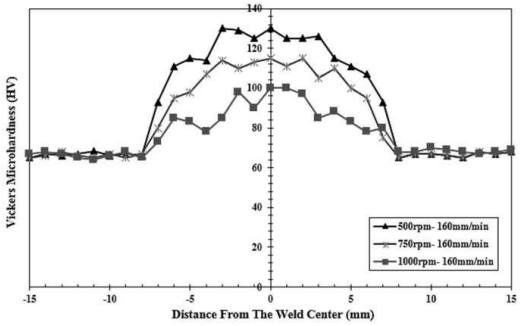

Fig. 7- The Image of the Vickers hardness test for alloy AA2024 [43].

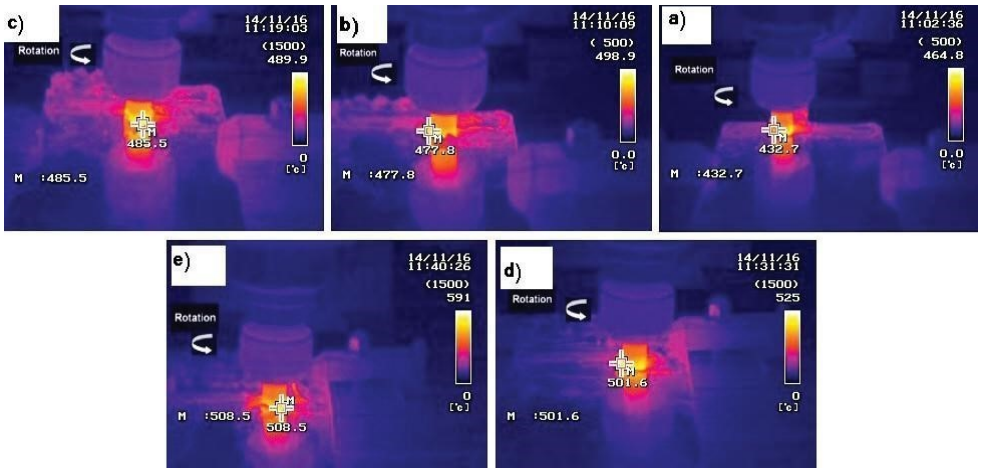

Fig. 8- The effect of tool rotational speed on the surface where the tool touches the workpiece. a) 600rpm, b) 800rpm, c) 1250rpm, d) 1600rpm, and e) 2000rpm [44].

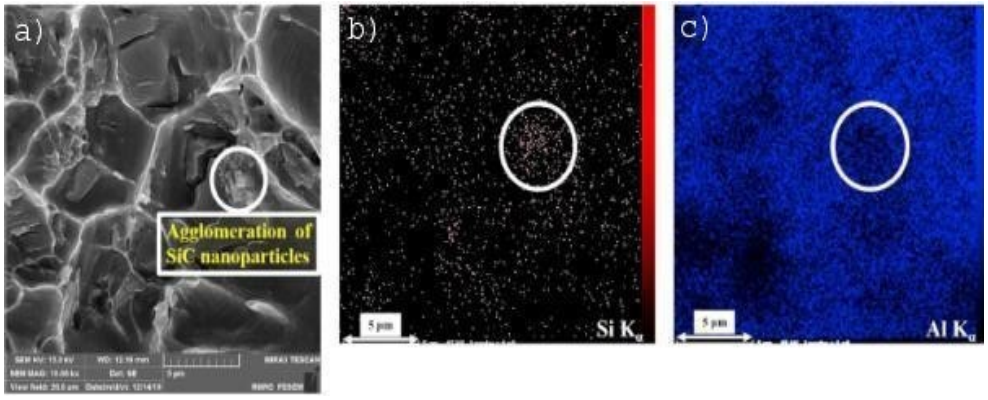

Fig. 9- FESEM image of the surface defect, b & d) the agglomeration of Sic nanopowders in AA5083 [45].

infrared images of thermal changes in the surface where the pin and the workpiece touch each other, respectively. The hardness increases by decreasing the toll rotational speed.

The temperature increases with the tool's rotational speed in the first occurrence, leading to grain growth. The second occurrence involves material flow improvement as the material transfer rate from the advancing side to the retreating side in the traverse zone increase by heightening the rotational speed. As a result, the materials mix well in the stir zone.

The third occurrence, which the incorrect rotational speed could cause, is related to using nanomaterial. The nanoparticles will be dispersed around the stir zone if the rotational speed exceeds an average rate. They will be agglomerated, just like in the research conducted by Mathur et al. [38], in which they covered TiO2 particles on the surface of AA5052 at a rotational speed of 1300rpm.

Rahmatian et al. [45] selected an incorrect tool rotational speed, leading to SiC nanoparticle agglomerating in TMAZ. As shown in Figure 9, the imaging of the defect location revealed that the agglomeration of SiC nanopowders causes stress concentration and thus defects in the sample.

b) Traverse Speed (mm/min): As illustrated in Table 2, the tool movement speed directly affects the microstructure in the stir zone.

As shown in Figure 10, the tool movement speed is directly correlated with the grain size. Based on the Hall–Petch equation, the smaller

Table 2- The effect of the tool rotational speed and the welding speed on microstructure in FSW and FSP

Consuming materials	Variable	Conclusion	Article authors	Year of publication	References
AA2024 Aluminium Alloys	500-1000rpm	As the tool rotates at FSW, the finer structure and stiffness increase.	Alvand et al.	2018	[43]
Composite AA6061	400-700rpm 150-500 mm/min	The tool rotational speed has a direct effect on Al_2O_3 nanoparticles with better bonding between the nanoparticles and the matrix.	Marzoli et al.	2006	[46]
AA 7020-T53	900-1400rpm 16-40 mm/min	Tool rotational speed in FSW has a direct effect on temperature.	Jweeg et al.	2012	[47]
Al6061-Al5083	700-2500rpm 25-400 mm/min	As the tool rotates and moves at FSW, the percentage of the material composition increases.	Ghaffarpour et al.	2012	[48]
Stainless Steel 304-6061 Al Alloy	560-900rpm	Due to the good combination of 304 Stainless Steel with Al, the hardness of the welding nugget part increases in FSW.	Ghosh et al.	2013	[49]
Aluminum Alloys	450-710rpm 20-40 mm/min	The finer structure and stiffness increase with the simultaneous growth of rotational tool speed and movement speed in FSP.	Balos et al.	2017	[50]
Al. Sic composite	700-1000rpm	By increasing tool rotational speed in FSP, no surface defects were created, and particles were evenly distributed in the amplifier.	Butola et al.	2021	[51]

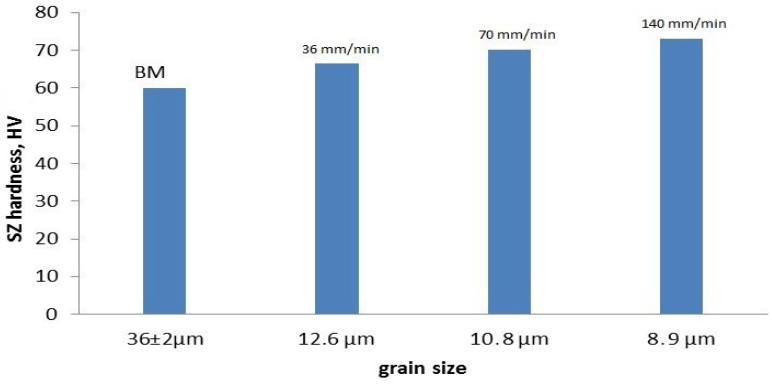

Fig. 10- The effect of tool movement speed on the grain size [54].

the grain size, the more hardness is expected. [52]. As the grain size gets smaller, obstacles will hinder the movement of dislocations; therefore, the material strengthens in the stir zone [53]. The hardness of the stir zone increases with a rise in the tool movement speed [54].

Lin et al., [55] analyzed the speed of FSW tool movement on Al–Zn–Mg alloys. They found out that the heat generated from severe plastic strain due to an increase in the tool movement speed causes a reduction in the grain size.

Input heat: By controlling the Input heat, the structure in the weld zone can be more coarse-grained or fine-grained [56]. Moreover, by accelerating the cooling rate of the stir zone, grain growth to have finer grain sizes can be prevented [57].

Kocańda et al. [58] believed that the highest portion of input heat on the workpiece surface is related to the frictional force between the tool's rotational speed and base metal.

Numerous researchers measured the heat produced by the friction of tools using, for example, a thermocouple or calculated the input heat through software design. By comparing the linear extrapolation, the multiple linear regression, and the multivariate Lagrange interpolation methods with the actual temperature of the stir zone, Yousefieh et al. [59] reported that the multivariate Lagrange interpolation method shows a closer estimation of the actual temperature in the stir zone compared to other methods.

According to Buffa et al. [60], an increase in FSW tool rotational speed force base metal grains to rotate in the broader direction with the rotational tool and to bear the more significant strain. An increase in the tool rotational speed increases the process's input heat and the size of recrystallized grains due to grain growth at high temperatures. Additionally, it causes the base metal to bear greater strain during FSW. Tufaro et al. [61] stated that increasing the input heat temperature decreases the hardness.

c) Tool Geometry and Design: Tool geometry is primary in achieving adequate microstructures in the stir and heat-affected zones. As illustrated in Figure 11, FSW and FSP tools consist of several parts, each of which needs to be designed [62].

Different pins affect the microstructure differently. As depicted in Figure 12, grain size changes in compliance with pin shape that affects the heat generated, and this heat has a direct effect on the structure of the stir zone, i.e., causing a structure to be more delicate in the base compared to the other bases [63].

According to Sadeesh et al. [64], it is possible to increase welding surface quality and the hardness in the weld zone by changing the pin shape, rotational tool speed, and welding movement speed. Emamian et al. [65] used several pins for FSW and reported that threaded pins affect mechanical properties and square pins increase

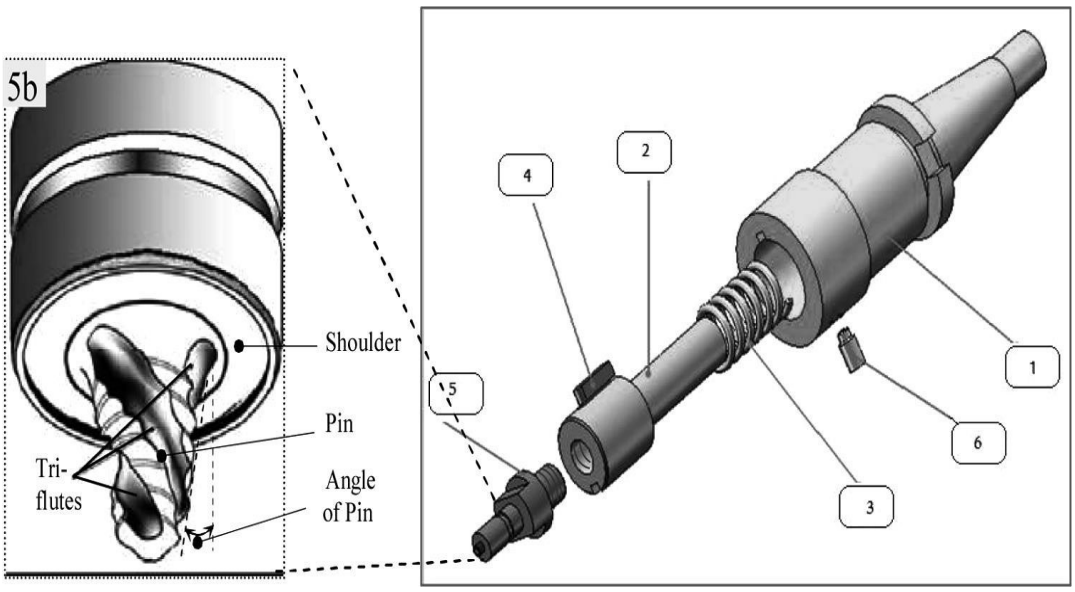

Fig. 11- Different tool parts [62].

input heat rate. Moreover, using cylindrical threaded pins results in better joints. Ullegaddi et al. [66] reported that the shoulder and the pin would provide the heat needed for material flow during FSW, making the structure of the stir zone finer or coarser by choosing the proper tools. Khan et al. [67] achieved new relations by measuring the pin length in FSW.

d) The Number of Passes in FSW and FSP: The more passes are, the finer and more uniform the structure can be obtained. An increase in the number of passes prevents the agglomeration of nanoparticles and causes a uniform distribution of nanoparticles. The effect of the number of passes on the structure of AA6082 can be seen in Figure 13 [68].

K. S. Wang et al. [69], W. Wang et al. [70], and Mabuwa et al. [71] showed that by increasing the number of FSP passes in the stir zone; the structure becomes finer after each pass and hardness increases as well.

As seen in the microscope image of AA6082, the grains of the base metal become finer and more organized after FSW, and ultimately, the structure becomes finer than before. This grain refinement increases hardness in the stir zone.

Dragatogiannis et al. [72] welded 5083 and 6082 aluminum alloys to each other by adding T nanoparticles. After three passes of FSP, the nanoparticles are distributed correctly in the stir zone, increasing the joint's hardness and mechanical properties.

Madhu et al. [73] and Mustafa et al. [74], if the number of passes in the stir zone increases, the structure will be finer, and the distribution of nanoparticles will be more uniform after each pass. Besides, the agglomeration of nanoparticles will be prevented, and hardness will increase.

The proper distribution of nanoparticles in FSW and FSP plays a significant role in determining the properties of the stir zone.

Singh et al. [75] analyzed the proper distribution of Al2O3 nanoparticles in 6061-T6 aluminum alloy. It was revealed that FSW plays a pivotal role in how nanoparticles are distributed and in increasing the hardness of the stir zone through nanoparticles. By adding SiO2 and Al2O3 nanoparticles to AA7075-T6 aluminum

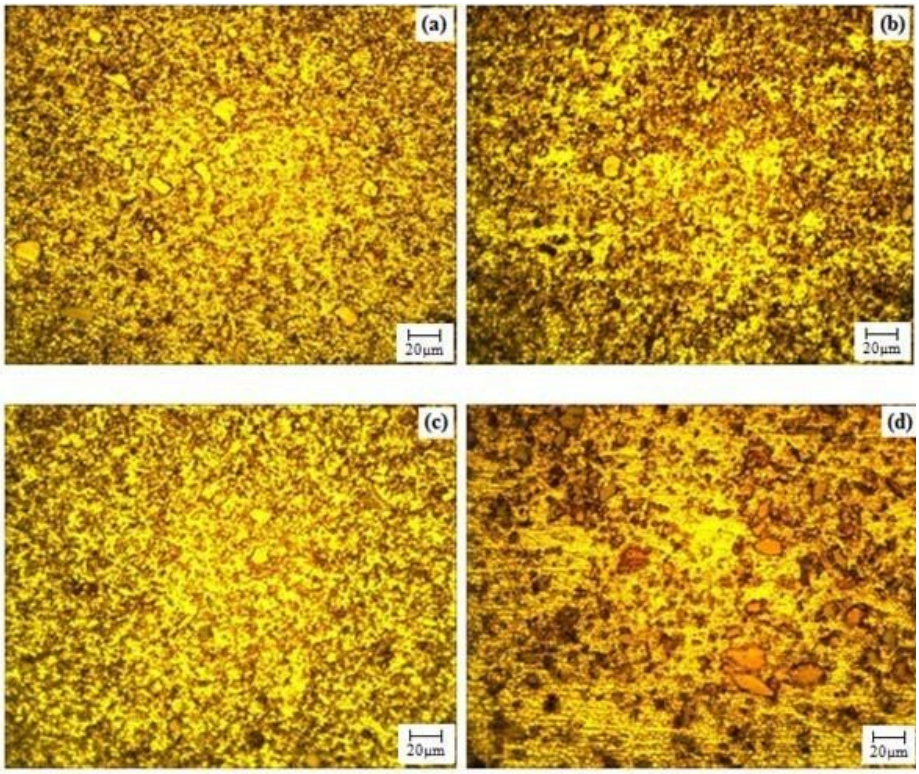

Fig. 12- Effect of tool pin profiles on FSP region microstructure in (a) Straight cylindrical, (b) Taper cylindrical, (c) Threaded cylindrical, and (d) Square samples [63].

alloy, Rashed et al. [76] managed to increase the hardness by 15-35% compared to the base metal using FSP because of the proper distribution of nanoparticles after three passes and the grain refinement of the stir zone. Table 3 demonstrates the studies of other researchers in this area.

5. Applications of FSW and FSP

Structure modification is one of the most significant applications of FSW and FSP. It is also possible to increase or decrease the properties of the base metal.

FSW welding is used for welding UFG aluminum alloys that are heat-sensitive and consist of unstable grain boundaries. FSP can be used to modify the structure after welding [82]. Yousefieh et al. [34] managed to weld an Al-0.2wt.% Sc properly alloy by increasing the tool's rotational speed. Before welding, the base metal was refined through the ARB process, and they then managed to make the structure of the stir zone finer using FSW. Sajuri et al., [83] first welded AA5083 sheets using FSW. After that, the sheets experienced cold rolling to increase hardness and uniformity. It was revealed that the hardness of the base metal increase by reducing its thickness, and the grain size dwindles. Using FSP, Mehdi et al., [84] modified the zone's structure welded by TIG so that the defects caused in the welded structure by fusion welding could be eliminated after FSP.

Additionally, the hardness can be increased by further refining. After cold spray coating, Huang et al. [85] used FSP. They reported that the structure of the coating became thinner, and Sic particles in the coating were uniformly

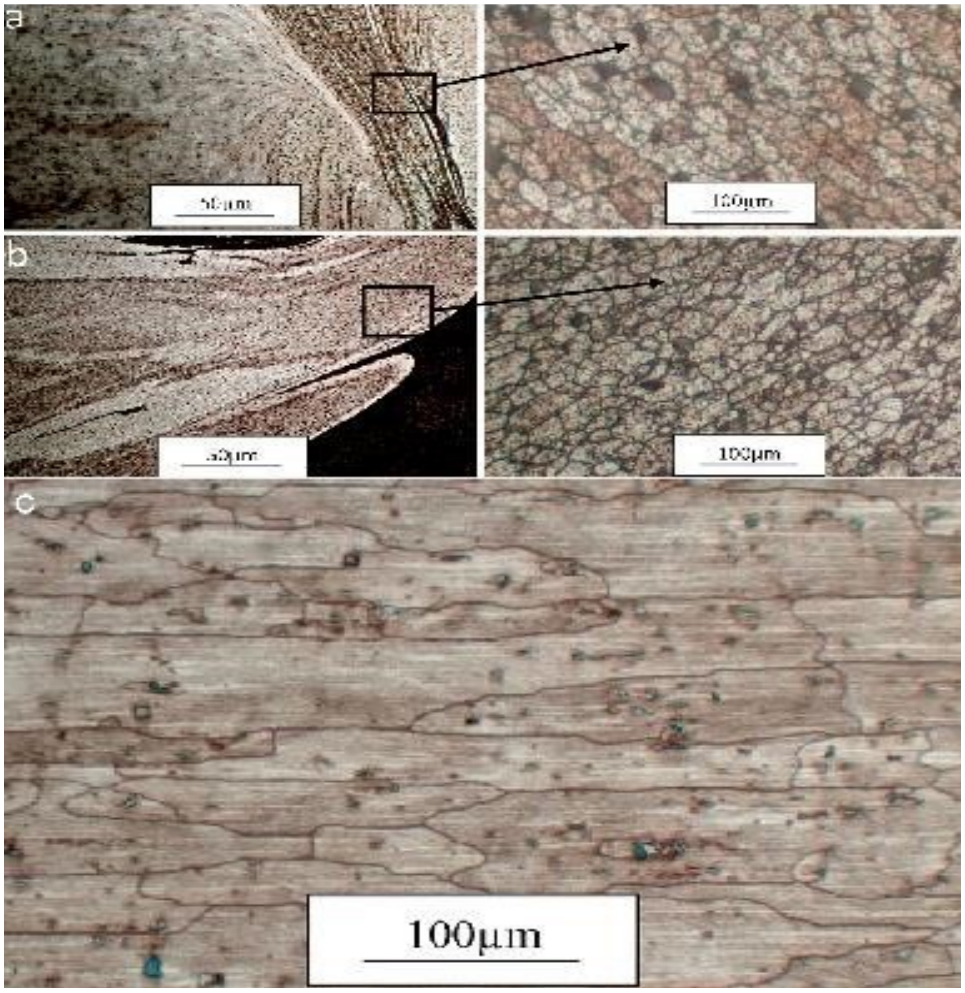

Fig. 13- Microscope images of the structure. a) AA6082 after FSW, b) A6082 after FSP, c) image of the base metal AA6082-T6 [68].

distributed in their bed.

Using FSW, Tabasi et al. [87] welded 7075-T6 aluminum alloy to AZ31 magnesium alloy by adding SiC nanoparticles. Mohammad et al. [86] added Al2O3 particles with a mean size of 3050nm to AA6082-T6 aluminum alloy with a 2 mm thickness. After three passes of FSW, the results showed that the nanoparticles have a more suitable distribution and a decrease in the grain size is observed in the stir zone. These factors lead the stir zone to be hardened.

Using friction stir welding can weld two dissimilar alloys. Reviewing the texture and microstructure of the two aluminum alloys in the stir zone, friction stir welding in a cube texture [001] often creates shear textures [123]. Therefore, a shear texture is predominant as the material flow in the stir zone is controlled by rotational and shear deformation. Moreover, the structure is finer and equiaxed in the stir zone under dynamic crystallization and grain refinement [88].

6. Visions and Challenges

Developing the processes mentioned in this analysis indicates a rational understanding of physical friction, and the associated mechanism is accessible in advance. The stir-based technologies primarily aim to achieve a sufficient level of material plasticity in the stir zone, allowing the dispersion and mixing of materials and the proper distribution of nanoparticles regardless of their compatibility. To achieve a coarse-grained or fine-grained structure, sufficient heat generation is necessary.

In several studies conducted, it was reported that the solid-state processes are more compatible and cost-efficient in terms of technical feasibility and product manufacturing quality based on the manufacturing of aluminum alloys, nanocomposites, composites, and other matters that need to be analyzed.

FSP can produce nanocomposites and composites of metal without changing the chemical compound. According to Table 3, FSP

Table 3- Appropriate distribution of nanoparticles in FSP and FSW

Article authors	Year of publication	Consuming materials	Process type	Conclusion	References
Patil et al.	2021	AA7075-Ti composite	FSP	TiC.Gr particles distribute uniformly across the composite surface.	[36]
Shinoda et al.	2004	Aluminum alloys	FSP	The distribution of the reinforcing phase is homogenous in the stir zone. This homogeneity affects mechanical and tribological properties because the final number of grains increases drastically in the reinforcement step.	[77]
Uzun et al.	2006	AA2124- Sic composite	FSW	SiC particles distribute correctly in the welded zone of the composite.	[78]
Bauri et al.	2011	Alzzomposite	FSP	TiC particles distribute uniformly across the composite surface.	[79]
Zhao et al.	2015	AA 6061 – B_4C composite	FSP	B_4C particles are properly distributed in the weldingzone, and increasing the the number of passes makes the distribution of particles in the welding zone more uniform.	[80]
Farahmand Nikoo et al.	2016	AA6061- T6.Al_2O_3 nanocomposite	FSW	Al_2O_3 nanoparticles distribute uniformly in the weld zone, and grain size in the stir zone decreases.	[81]

is extremely useful in producing nanocomposites and must be further investigated.

In 2xxx and 6xxx aluminum alloys, the second phase particles prevent the grain growth and mobility of dislocations, affecting the particles' sedimentation and dynamic growth. By controlling the rotation speed and heat input, one can improve the mechanical properties of these alloys. With one pass of FSP on the surface of the processed area, the structure of the surface is fine-grained. Also, FSP can be used selectively, that is, in parts of the part that require superplastic deformation and, therefore, the need for fine graining is used if this is not possible in other SPD methods. In FSP.FSW, the increase in temperature directly affects superplasticity, and with temperature control, which requires control of tool movement speed, the number of passes, etc. The researchers can use alloy elements to form pinning particles to control grain size. The researchers know superplasticity involves dynamic grain growth, and this issue should be considered more seriously. Moreover, the effects of deformation temperature and strain rate on the thermally activated grain boundary sliding (GBS), precipitation of secondary phases (especially the Cr-rich σ phase), dissolution of phases, deformation-induced (dynamic) grain growth, partial melting, and high strain rate superplasticity by the friction stir processing are among the challenges that some researchers have addressed. [8, 13, 29, 89, 90].

7. Summary

With the help of all the information gathered about FSW and FSP by different researchers, it can be concluded that with an increase in the rotational speed of materials in the stir zone, the particles mix uniformly. Hardness increases by heightening the movement speed of tools. A rise in the tool's rotational speed reduces hardness. With increased traverse speed, input heat increases from a special rate to an optimized rate, leading to grain growth and low hardness. Moreover, a simultaneous increase in tool rotational speed and movement speed leads to a more proper mixture and stir of materials and a finer microstructure of various zones.

Additionally, the present study revealed that FSP could be used to modify the surface of composites, manufacture MCCs, and distribute nanoparticles uniformly in joints or across the coating surface. FSW and FSP change the structure of aluminum and aluminum alloys. In the case of rolled alloys, the structure of the grains changes from an elongated form in the direction of rolling to a completely equiaxed form. Implementing refrigerant conditions during the process by absorbing the heat generated through pin rotation and its stir reduces the mechanism of grain growth and the final grain size. The structure becomes more equiaxed and finer with each FSW and FSP pass, and its hardness increases. According to the results, the equiaxed coarse grains turned into the equiaxed fine grains during FSW and FSP. Grain refinement caused by FSW and FSP could be due to dynamic phenomena. According to the simultaneous presence of plastic deformation and high heat during the process, recovery, and dynamic recrystallization they occurred in the stir zone. Using nanoparticles increases the properties of the weld zone. By increasing the number of passes in FSW and FSP, nanomaterials dispersed more appropriately in the stir zone, improving tensile strength and hardness. By increasing the number of passes in FSW and FSP, the agglomeration of nanomaterial in and around the stir zone decreased.

References

1. E. Ghali, Corrosion resistance of aluminum and magnesium alloys: understanding, performance, and testing, John Wiley & Sons2010.

2. G.E. Totten, D.S. MacKenzie, Handbook of aluminum: vol. 1: physical metallurgy and processes, CRC press2003.

3. P. Vishnu, R.R. Mohan, E.K. Sangeethaa, S. Raghuraman, R. Venkatraman, A review on processing of aluminium and its alloys through Equal Channel Angular Pressing die, Materials Today: Proceedings 21 (2020) 212-222.

4. J.C. Lee, S.H. Lee, S.W. Kim, D.Y. Hwang, D.H. Shin, S.W. Lee, The thermal behavior of aluminum 5083 alloys deformed by equal channel angular pressing, Thermochimica acta 499(1-2) (2010) 100-105.

5. A.H. Seikh, M. Baig, A.U. Rehman, F.H. Hashmi, J.A. Mohammed, Stress Corrosion Cracking Behavior of Fine-Grained Al5083 Alloys Processed by Equal-Channel Angular Pressing (ECAP), Molecules 26(24) (2021) 7608.

6. J. Fahim, S. Hadavi, H. Ghayour, S.H. Tabrizi, Cavitation erosion behavior of super-hydrophobic coatings on Al5083 marine aluminum alloy, Wear 424 (2019) 122-132.

7. K. Edalati, A. Bachmaier, V.A. Beloshenko, Y. Beygelzimer,

V.D. Blank, W.J. Botta, K. Bryła, J. Čížek, S. Divinski, N.A. Enikeev, Nanomaterials by severe plastic deformation: review of historical developments and recent advances, Materials Research Letters 10(4) (2022) 163-256.

8. M.S. Khorrami, A. Mirzaei, F. Azadi, R. Peymanfar, M. Yektaei, S. Javanshir, A. Shafiei-Zarghan, A. Najafi, S.F. Kashani-Bozorg, A. Zarei-Hanzaki, Friction stir welding of ultrafine grained aluminum alloys: a review, Journal of Ultrafine Grained and Nanostructured Materials 54(1) (2021) 1-20.

9. R.Y. Lapovok, The role of back-pressure in equal channel angular extrusion, Journal of materials science 40 (2005) 341-346.

10. S.-Y. Chang, J.G. Lee, K.-T. Park, D.H. Shin, Microstructures and mechanical properties of equal channel angular pressed 5083 Al alloy, Materials Transactions 42(6) (2001) 1074-1080.

11. H. Zendehdel, A. Hassani, Influence of twist extrusion process on microstructure and mechanical properties of 6063 aluminum alloy, Materials & Design 37 (2012) 13-18.

12. G. Faraji, E. Taherkhani, M.R. Sabour, Cyclic severe plastic deformation processes, (2023).

13. M. AAli, G. Faraji, M.R. Sadrkhah, A. Fata, M.J. Hadad, Evaluation of Microstructure and Tensile Behavior of Fine-Grained AZ61 Alloy Tube Processed by Severe Plastic Deformation, Journal of Advanced Materials and Processing 7(3) (2019) 53-62.

14. S. Hadi, M.H. Paydar, Investigation on the properties of high pressure torsion (HPT) processed Al/B4C composite, Journal of Ultrafine Grained and Nanostructured Materials 53(2) (2020) 146-157.

15. V. Segal, The method of material preparation for subsequent working, Patent of the USSR 575892 (1977) 330.

16. A. Esbolat, E. Panin, A. Arbuz, A. Naizabekov, S. Lezhnev, A. Yerzhanov, I. Krupenkin, I. Volokitina, A. Volokitin, Development of Asymmetric Rolling as a Severe Plastic Deformation Method: A Review, Journal of Ultrafine Grained and Nanostructured Materials 55(2) (2022) 97-111.

17. G. Faraji, H.S. Kim, H.T. Kashi, Severe plastic deformation: methods, processing and properties, Elsevier2018.

18. H. Miyamoto, Corrosion of ultrafine grained materials by severe plastic deformation, an overview, Materials Transactions 57(5) (2016) 559-572.

19. K. Kutniy, I. Papirov, M. Tikhonovsky, A. Pikalov, S. Sivtzov, L. Pirozhenko, V. Shokurov, V. Shkuropatenko, Influence of grain size on mechanical and corrosion properties of magnesium alloy for medical implants, Materialwissenschaft und Werkstofftechnik: Entwicklung, Fertigung, Prüfung, Eigenschaften und Anwendungen technischer Werkstoffe 40(4) (2009) 242-246.

20. T. Mahmoud, Effect of friction stir processing on electrical conductivity and corrosion resistance of AA6063-T6 Al alloy, Proceedings of the Institution of Mechanical Engineers, Part C: Journal of Mechanical Engineering Science 222(7) (2008) 1117-1123.

21. Y. Li, F. Wang, G. Liu, Grain Size Effect on the Electrochemical Corrosion Behavior of Surface Nanocrystallized Low-Carbon Steel, October 2004, Corrosion 60(10) (2004).

22. N. Birbilis, K. Ralston, S. Virtanen, H. Fraser, C. Davies, Grain character influences on corrosion of ECAPed pure magnesium, Corrosion Engineering, Science and Technology 45(3) (2010) 224-230.

23. S. Wang, C. Shen, K. Long, H. Yang, F. Wang, Z. Zhang, Preparation and electrochemical corrosion behavior of bulk nanocrystalline ingot iron in HCl acid solution, The Journal of Physical Chemistry B 109(7) (2005) 2499-2503.

24. S. Tao, D. Li, Tribological, mechanical and electrochemical properties of nanocrystalline copper deposits produced by pulse electrodeposition, Nanotechnology 17(1) (2005) 65.

25. K. Ralston, N. Birbilis, Effect of grain size on corrosion: a review, Corrosion 66(7) (2010) 075005-075005-13.

26. H. Nakano, S. Oue, S. Taguchi, S. Kobayashi, Z. Horita, Stress-corrosion cracking property of aluminum-magnesium alloy processed by equal-channel angular pressing, International Journal of Corrosion 2012 (2012).

27. A.H. Seikh, M. Baig, A. Ur Rehman, Effect of Severe Plastic Deformation, through Equal-Channel Angular Press Processing, on the Electrochemical Behavior of Al5083 Alloy, Applied Sciences 10(21) (2020) 7776.

28. R.Z. Valiev, T.G. Langdon, Principles of equal-channel angular pressing as a processing tool for grain refinement, Progress in materials science 51(7) (2006) 881-981.

29. Z. Horita, T. Fujinami, M. Nemoto, T. Langdon, Improvement of mechanical properties for Al alloys using equal-channel angular pressing, Journal of Materials Processing Technology 117(3) (2001) 288-292.

30. M. Reihanian, R. Ebrahimi, N. Tsuji, M. Moshksar, Analysis of the mechanical properties and deformation behavior of nanostructured commercially pure Al processed by equal channel angular pressing (ECAP), Materials Science and Engineering: A 473(1-2) (2008) 189-194.

31. R. Jamaati, M.R. Toroghinejad, High-strength and highly-uniform composite produced by anodizing and accumulative roll bonding processes, Materials & Design 31(10) (2010) 4816-4822.

32. M. Eftekhari, G. Faraji, M. Bahrami, Processing of commercially pure copper tubes by hydrostatic tube cyclic extrusion–compression (HTCEC) as a new SPD method, Archives of Civil and Mechanical Engineering 21(3) (2021) 1-12.

33. M. Eftekhari, A. Fata, G. Faraji, M.M. Mashhadi, Hot tensile deformation behavior of Mg-Zn-Al magnesium alloy tubes processed by severe plastic deformation, Journal of Alloys and Compounds 742 (2018) 442-453.

34. A. Fattah-alhosseini, A.R. Ansari, Y. Mazaheri, M. Karimi, M. Haghshenas, An Investigation of mechanical properties in accumulative roll bonded nano-grained pure titanium, Materials Science and Engineering: A 688 (2017) 218-224.

35. M.Y. Alawadhi, S. Sabbaghianrad, Y. Huang, T.G. Langdon, Direct influence of recovery behaviour on mechanical properties in oxygen-free copper processed using different SPD

techniques: HPT and ECAP, Journal of Materials Research and Technology 6(4) (2017) 369-377.

36. M.M. Sharma, C.W. Ziemian, Pitting and stress corrosion cracking susceptibility of nanostructured Al-Mg alloys in natural and artificial environments, Journal of materials engineering and performance 17 (2008) 870-878.

37. I.-J. Son, H. Nakano, S. Oue, S. Kobayashi, H. Fukushima, Z. Horita, Pitting corrosion resistance of ultrafine-grained aluminum processed by severe plastic deformation, Materials Transactions 47(4) (2006) 1163-1169.

38. T. Tański, P. Snopiński, P. Nuckowski, T. Jung, W. Kwaśny, T. Linek, Influence of processing routes on structure and residual stress in aluminium-magnesium alloy after ECAP, Journal of Achievements in Materials and Manufacturing Engineering 63(1) (2014) 5-12.

39. E. B. Moustafa, W. S. Abushanab, A. Melaibari, A. V. Mikhaylovskaya, M. S. Abdel-Wahab, and A. O. Mosleh, "Nano-surface composite coating reinforced by Ta2 C, Al2 O3 and MWCNTs nanoparticles for aluminum base via FSP," Coatings, 2021; 11(12). doi: 10.3390.coatings11121496.

40. F. Ostovan, S. Amanollah, M. Toozandehjani, and E. Shafiei, "Fabrication of Al5083 surface hybrid nanocomposite reinforced by CNTs and Al2O3 nanoparticles using friction stir processing," J of Composite Mater, 2020; 54(8), 1107–1117. doi: 10.1177.0021998319874849.

41. M. Yousefieh, M. Tamizifar, S. M. A. Boutorabi, and E. Borhani, "Optimization of friction stir welding parameters for mechanical properties of Nano.UFG Aluminum- scandium alloys by using design of experiment method," JWSTI, 2018; 3(2),79-89.

42. S. S. M. Mehrian, M. Rahsepar, F. Khodabakhshi, and A. P. Gerlich, "Effects of friction stir processing on the microstructure, mechanical and corrosion behaviors of an aluminum-magnesium alloy," Surface and Coatings Technology, 2021; 405. doi: 10.1016.j.surfcoat.2020.126647.

43. M. Alvand, H. Abdollah-Pour, E. Borhani, and M. Naseri "Effect of rotational and welding speeds on microstructure and mechanical properties of friction stir welded AA2024 aluminum sheets."8th Congress & 3rd International Eng Mater & Metallurgy, 2014; 18-19.

44. M. Fekri Soostani, R. Taghiabadi, M. Jafarzadegan "Improving the mechanical properties of Al-Ni-Fe alloys through friction stir processing," MetallurgicalEngineering,2017; 20(2), 121-131. doi: http:..dx.doi.org. 10.22076.me.2017.63859.1136.

45. B. Rahmatian, K. Dehghani, and S. E. Mirsalehi, "Effect of adding SiC nanoparticles to nugget zone of thick AA5083 aluminum alloy joined by double-sided friction stir welding," J of Manufacturing Processes, 2020; 52(2019), 152–164. doi: 10.1016.j.jmapro.2020.01.046.

46. L. M. Marzoli, A. V. Strombeck, J. F. Dos Santos, C. Gambaro, and L. M. Volpone, "Friction stir welding of an AA6061. Al2O3.20p reinforced alloy," Composites Science and Technology, 2006; 66(2). doi: 10.1016.j.compscitech.2005.04.048.

47. M. Jweeg, M. H. Tolephih, M.A. Sattar, "EFFECT OF FRICTION STIR WELDING PARAMETERS (ROTATION AND TRANSVERSE) SPEED ON THE TRANSIENT TEMPERATURE DISTRIBUTION IN FRICTION STIR WELDING OF AA 7020-T53," ARPN Journal of Engineering and Applied Sciences, 2012; 7(4).

48. M. Ghaffarpour, B. M. Dariani, A. Hossein Kokabi, and N. A. Razani, "Friction stir welding parameters optimization of heterogeneous tailored welded blank sheets of aluminum alloys 6061 and 5083 using response surface methodology," Proceedings of the Institution of Mechanical Engineers, Part B: Journal of Engineering Manufacture, vol. 226, no. 12, 2012, doi: 10.1177.0954405412461864.

49. M. Ghosh, R. K. Gupta, and M. M. Husain, "Friction stir welding of stainless steel to al alloy: Effect of thermal condition on weld nugget microstructure," Metallurgical and Materials Transactions A: Physical Metallurgy and Materials Science, vol. 45, no. 2, 2014, doi: 10.1007.s11661-013-2036-9.

50. S. Balos, D. L. Zlatanovic, P. Janjatovic, M. Dramicanin, D. Rajnovic, and L. Sidjanin, "Wear Resistance Increase by Friction Stir Processing for Partial Magnesium Replacement in Aluminium Alloys," in IOP Conference Series: Materials Science and Engineering, 2018, vol. 329, no. 1, doi: 10.1088.1757-899X.329.1.012017.

51. R. Butola, L. Tyagi, R. M. Singari, Q. Murtaza, H. Kumar, and D. Nayak, "Mechanical and wear performance of Al.SiC surface composite prepared through friction stir processing," Materials Research Express, vol. 8, no. 1, 2021, doi: 10.1088.2053-1591.abd89d.

52. R. W. Armstrong, "Hall-Petch Relationship : Use in Characterizing Properties of Aluminum and Aluminum Alloys*," Materials Science, 2016; Corpus ID: 37797939.

53. M. Khoobroo, A. Maleki, B. Niroumand, "Improving the Surface Properties of Gray Cast Iron through In-Situ Alloying," Journal of Advanced Materials in Engineering, 2017; 36 (3), 1–10. DOI:10.29252.JAME.36.3.1,Corpus ID: 139113259.

54. M. M. El Rayes, M. S. Soliman, A. T. Abbas, D. Y. Pimenov, I. N. Erdakov, and M. M. Abdel-Mawla, "Effect of Feed Rate in friction stir welding on the Mechanical and Microstructural Properties of AA5754 Joints," Advances in Mater Sci and Eng, 2019; (12). doi: 10.1155.2019.4156176.

55. Sen Lin, Jianguo Tang, Shengdan Liu, Yunlai Deng, Huaqiang Lin, Hua Ji, Lingying Ye, Xinming Zhang, "Effect of travel speed on microstructure and mechanical properties of FSW joints for Al-Zn-Mg alloy," Materials, 2019; 12(24). https:.. doi.org.10.3390.ma12244178.

56. J. J. Shen, H. J. Liu, and F. Cui, "Effect of welding speed on microstructure and mechanical properties of friction stir welded copper," Mater and Design, 2010; 31(8),3937–3942. doi: 10.1016.j.matdes.2010.03.027.

57. S. Yahya Abadi, M. Abbasi, "Modification of Mechanical Properties of Al6061 Aluminum Alloy Joint Formed Using Friction Stir Welding by Increasing the Cooling Rate and Application of Vibration," Modares Mechanical Engineering, 2019, 19(6), 1551-1558.

58. D. Kocańda, A. Górka, and D. Zasada, "Formation of a Metal Coating by Means of Friction Stir Processing," ICAF 2011 Structural Integrity: Influence of Efficiency and Green Imper-

atives,2011.

59. M. Yousefieh, A. Jabbari, "Modeling of temperature in friction stir welding of duplex stainless steel using multivariate lagrangian methods, linear extrapolation, and multiple linear regression," JWSTI, 2020; 6 (2),65-76.

60. G. Buffa, G. Campanile, L. Fratini, and A. Prisco, "Friction stir welding of lap joints: Influence of process parameters on the metallurgical and mechanical properties," Materials Science and Engineering A, 2009; 519(1–2), 19–26. doi: 10.1016.j.msea.2009.04.046.

61. L. N. Tufaro, I. Manzoni, and H. G. Svoboda, "Effect of Heat Input on AA5052 Friction Stir Welds Characteristics," Procedia Mater Sci, 2015; 8, 914–923. doi: 10.1016.j.mspro.2015.04.152.

62. M. Aissani, S. Gachi, F. Boubenider, and Y. Benkedda, "Design and optimization of friction stir welding tool," Mater and Manufacturing Processes, 2010; 25(11). doi: 10.1080.10426910903536733.

63. John Baruch L, R. Raju, and V. Balasubramanian, "Effect of Tool Pin Profile on Microstructure and Hardness of Friction Stir Processed Aluminum Die Casting Alloy Study," European Journal of Scientific Research, 2012;70(3),375-385.

64. P. Sadeesh, M.VenkateshKannan, V.Rajkumar, P.Avinash, N.Arivazhagan, K.Devendranath Ramkumar, S.Narayanan, "Studies on friction stir welding of aa 2024 and aa 6061 dissimilar metals," in Procedia Engineering, 2014; 75. doi: 10.1016.j.proeng.2013.11.031.

65. S. Emamian, M. Awang, P. Hussai, B. Meyghani, and A. Zafar, "Influences of tool pin profile on the friction stir welding of AA6061," ARPN J of Eng and Applied Scis, 2016; 11(20).

66. K. Ullegaddi, V. Murthy, R. N. Harsha, and Manjunatha, "Friction Stir Welding Tool Design and Their Effect on Welding of AA-6082 T6," Mater Today: Proceedings, 2017; 4(8). doi: 10.1016.j.matpr.2017.07.133.

67. N. Z. Khan, A. N. Siddiquee, and Z. A. Khan, "Proposing a new relation for selecting tool pin length in friction stir welding process," Journal of the International Measurement Confederation, 2018; 129, 112–118. doi: 10.1016.j.measurement.

68. V. Msomi and S. Mabuwa, Analysis of material positioning towards microstructure of the friction stir processed AA1050. AA6082 dissimilar joint," Advances in Industrial and Manufacturing Eng, 2020; 1. doi: 10.1016.j.aime.2020.100002.

69. K. S. Wang, W. Guo, W. Wang, and W. L. Wang, "Effect of accumulation of friction stir processing on microstructure and properties of cast pure aluminum L2," Hangkong Cailiao Xuebao.Journal of Aeronautical Materials, 2009; 29(5), 29–32.

70. W. Wang, K. Wang, Q. Guo, and N. Wu, "Effect of friction stir processing on microstructure and mechanical properties of cast AZ31 magnesium alloy," Xiyou Jinshu Cailiao Yu Gongcheng. Rare Metal Materials and Engineering,2012; 41(9), 1522–1526. doi: 10.1016.s1875-5372(13)60004-1.

71. S. Mabuwa, V. Msomi, "The effect of friction stir processing on the friction stir welded AA1050-H14 and AA6082-T6 joints," in Materials Today: Proceedings, 2019; 26. doi: 10.1016.j.matpr.2019.10.039.

72. D. A. Dragatogiannis, E. P. Koumoulos, I. A. Kartsonakis, D. I. Pantelis, P. N. Karakizis, and C. A. Charitidis, "Dissimilar Friction Stir Welding Between 5083 and 6082 Al Alloys Reinforced With TiC Nanoparticles," Materials and Manufacturing Processes, 2016; 31(16),2101–2114. doi: 10.1080.10426914.2015.1103856.

73. H. C. Madhu, P. Ajay Kumar, C. S. Perugu, and S. V. Kailas, "Microstructure and Mechanical Properties of Friction Stir Process Derived Al-TiO2 Nanocomposite," Journal of Materials Engineering and Performance, 2018; 27(3), 1318–1326.doi: 10.1007.s11665-018-3188-y.

74. E. Moustafa, "Effect of multi-pass friction stir processing on mechanical properties for AA2024.Al2O3 nanocomposites," Materials, 2017; 10(9). doi: 10.3390.ma10091053.

75. T. Singh, S. K. Tiwari, and D. K. Shukla, "Effects of Al2O3 nanoparticles volume fractions on microstructural and mechanical characteristics of friction stir welded nanocomposites," Nanocomposites,2020; 6(2), 76–84. doi: 10.1080.20550324.2020.1776504.

76. S. E.Rashed, H. A.Hassan, T. G.Abu-El-Yazied, A. B. El-Shabasy, "SURFACE IMPROVEMENT OF 7075 ALLOY USING FRICTION STIR," JOURNAL OF THE EGYPTIAN SOCIETY OF TRIBOLOGY, 2020; 17(2),1–12.

77. T. Shinoda, M. Kawai, H. Takegami, "NOVEL PROCESS OF SURFACE MODIFICATION OF ALUMINIUM CASTS APPLYING FRICTION STIR PHENOMENON," Materials Science,2005; DOI:10.1007.BF03266469, Corpus ID: 137169086

78. H. Uzun, "Friction stir welding of SiC particulate reinforced AA2124 aluminum alloy matrix composite," Materials and Design, 2007; 28(5).doi: 10.1016.j.matdes.2006.03.023.

79. R. Bauri, D. Yadav, and G. Suhas, "Effect of friction stir processing (FSP) on microstructure and properties of Al-TiC in situ composite," Materials Science and Engineering A, 2011; 528(13–140). doi: 10.1016.j.msea.2011.02.085.

80. Y. Zhao, X. Huang, Q. Li, J. Huang, and K. Yan, "Effect of friction stir processing with B4C particles on the microstructure and mechanical properties of 6061 aluminum alloy," International Journal of Advanced Manufacturing Technology, 2015; 78, (9–12). doi: 10.1007.s00170-014-6748-9.

81. M. Farahmand Nikoo, H. Azizi, N. Parvin, and H. Yousefpour Naghibi, "The influence of heat treatment on microstructure and wear properties of friction stir welded AA6061-T6. Al2O3 nanocomposite joint at four different traveling speed," Journal of Manufacturing Processes, 2016; 22, 90–98.doi: 10.1016.j.jmapro.2016.01.003.

82. M. Sarkari Khorrami," Friction stir welding of ultrafine grained aluminum alloys: a review", Journal of Ultrafine Grained and Nanostructured Materials, 2021; 54(1), 1-20. doi: 10.22059.jufgnsm.2021.01.01

83. Z. Sajuri et al., "Cold-rolling strain hardening effect on the microstructure, serration-flow behaviour and dislocation density of friction stir welded AA5083," Metals, 2020; 10(1). doi: 10.3390.met10010070.

84. H. Mehdi , R. S. Mishra, "Effect of Friction Stir Processing on Microstructure and Mechanical Properties of TIG Welded Joint

of AA6061 and AA7075," Defence Technology, 2021;17,715-727. doi: 10.1016.j.dt.2020.04.014

85. C. Huang et al., "Modification of a cold sprayed SiCp. Al5056 composite coating by friction stir processing," Surface and Coatings Technology, 2016; 296(69–75).doi: 10.1016.j.surfcoat.2016.04.016.

86. S. Mohammed and A. K. Birru, "Friction Stir Welding of AA6082 Thin Aluminium Alloy Reinforced with Al2O3 Nanoparticles," Transactions of the Indian Ceramic Society, 2019; 78(3),137–145. doi: 10.1080.0371750X.2019.1635046.

87. M. Tabasi, M. Farahani, M. K. B. Givi, M. Farzami, and A. Moharami, "Dissimilar friction stir welding of 7075 aluminum alloy to AZ31 magnesium alloy using SiC nanoparticles," International J of Advanced Manufacturing Technology, 2016; 86(1–4), 705–715. doi: 10.1007.s00170-015-8211-y.

88. B. Wang, B. B. Lei, J. X. Zhu, Q. Feng, L. Wang, and D. Wu, "EBSD study on microstructure and texture of friction stir welded AA5052-O and AA6061-T6 dissimilar joint," Mater and Design, 2015; 87, 593–599. doi: 10.1016.j.matdes.2015.08.060.

9. R. Motallebi, Z. Savaedi & H. Mirzadeh, "Superplasticity of high-entropy alloys: a review", Archives of Civil and Mechanical Engineering, 2022; 22. https:..doi.org.10.1007.s43452-021-00344-x.

90. H. Mirzadeh, " High strain rate superplasticity via friction stir processing (FSP): A review", Materials Science & Engineering A, 2021; 819, 141499. doi:10.1016.j.msea.2021.141499.